JOURNAL OF MATERIALS SCIENCE 20 (1985) 2586–2596

R-curve evaluation with ceramic materials at elevated temperatures by an energy approach using direct observation and compliance calculation of the crack length

A. BORNHAUSER
Institut für Nichtmetallische Werkstoffe, Technische Universität, D-1000 Berlin 12, West Germany

K. KROMP
Institut für Festkörperphysik, Universität Wien, Austria

R. F. PABST
Max-Planck-Institut für Metallforschung, Institut für Werkstoffwissenschaften, Stuttgart, West Germany

An experimental procedure is presented which allows the direct visual observation and measurement of crack extension in ceramic materials at high temperatures. The directly measured crack lengths, gained from displacement-controlled three-point bend tests, are compared to those calculated from the compliance. An energy approach is presented to calculate *R*-values from the load–displacement curves. These *R*-values for a pure alumina and an alumina containing a glassy phase, for which the load–displacement curves show non-linearity at high temperatures, are compared to *K*-values and *J*-values. The stress intensity approach, based on traction-free surfaces, gives unrealistic data for the non-linear behaving material owing to adhesive effects behind the actual crack front. The *J*-values, calculated by two methods developed for investigations with moving cracks, are identical to those from the energy approach.

1. Introduction

Ceramic materials are becoming increasingly important as high performance materials for engineering purposes. The successful application of ceramics, however, requires a knowledge of material characteristic crack extension properties which enable the designer to reasonably predict the material behaviour in service. Owing to their brittleness, ceramic materials seem best suited for linear elastic fracture mechanics measurements, the analytical developments coming through a continuum approach. At a linear elastic stage the LEFM-concept, therefore, yields reasonable material constants (K_{IC} data, v–K_I relationship) and often results in good agreement between different methods (e.g. DT test, bend test). Two main objections may be raised, however, in using the continuum linear elastic approach. First, the dangerous flaws in ceramic materials are as large as the microstructural components. From this it may be questioned whether continuum equations characterize their strength behaviour. Second, the stress–strain behaviour may become non-linear and applying linear elastic fracture mechanics could be problematic.

Observations suggest that the appearance of non-linearity is neither accompanied by a plastic zone, well defined in front of a crack tip, nor by macroscopic blunting effects as is the case with metallic materials. Consequently, the cracked

0022–2461/85 $03.00 + .12

surfaces behind the crack tip keep close together and are not traction free. It seems rational, therefore, to consider friction effects and adhesive forces at the crack surfaces.

"Plasticity" effects are mostly found at elevated temperatures. It should be mentioned, however, that even at room temperature, pronounced macroscopic non-linear stress–strain behaviour may be detected if coarse-grained materials with high internal stresses or high microcrack densities are slowly loaded.

Most of the plasticity effects can be attributed to the phenomenon of slow crack growth accompanied by secondary crack formation. In addition, at high temperatures "plasticity" effects due to viscous second-phase reactions may influence the stress–strain behaviour. Moreover, the strength and deformation not only depends on temperature but heavily on loading rate.

The susceptibility to secondary crack formation makes it difficult to define a reliable crack length. As for instance the stress intensity is defined only for a single well-defined crack, its applicability may be questioned if long parallel cracks develop.

The difficulties in defining an equivalent crack length and the "plasticity" effects summarized as: secondary crack formation, friction effects, adhesive forces with viscous reactions, seem to be obstacles for any evaluation of reliable critical or subcritical crack extension parameters.

Owing to the uncertainty in the definition of crack length together with friction and adhesive effects, the measured crack resistance values may depend not only on temperature and loading rate but also on the crack length itself, forming a so-called R-curve.

2. Energy concept and crack resistance

Referring to the "plasticity" effects, a J-integral formalism should be used to obtain relevant fracture parameters. This was done in a previous paper [1]. The methods established were quite analogous to those introduced with metallic materials [2, 3]. The single specimen compliance method (SSPCM) with partial and total unloading and the multiple specimen method (MSPM) both resulted in rising crack resistance curves, J_R, at elevated temperatures (J as a function of the normalized crack length, a/W) if an alumina with a glassy phase was used.

In the case of unloading this was attributed to crack closure due to viscous reactions and referring to the MSPM-method to subcritical crack extension as a function of crack length [1–3]. Those effects bring about that the recommended J-integral methods and the philosophy behind them may become problematic.

The J-value is defined for a stationary crack (excluding subcritical crack extension) where the non-linear stress–strain behaviour is traced back to a plastic zone in front of the crack and not to viscous, adhesive reactions eventually behind the actual crack front.

To avoid crack closure effects due to unloading, a completely deflection-controlled load–displacement curve should be performed which guarantees a stationary crack growth. The definition, calculation and measurement of crack length is then decisive.

Crack lengths may be calculated by the change in compliance, which includes both, subcritical crack elongation and viscous plasticity reactions. To separate the effects, direct visual observation and measurement of the crack length during the continuous loading process should be performed. The presumption is that the direct observation detects the separation of cracked surfaces but one cannot decide whether the cracked surfaces immediately behind the crack front are traction free or not.

In the following sections an analytical background is presented to define a parameter R characterizing the crack resistance of a stationary moving crack. R is chosen instead of a J-concept interpretation to avoid discussions concerning the definition of the J-integral.

Consider an elastic–plastic body (in this case a three-point bending specimen) containing a single plane crack of length a which has a traction free crack surface area $A = aB$ (a = crack length, B = specimen thickness). The crack may be propagated by energy supply in a stable, slow way, so that the crack acceleration is small and the kinetic energy of the body is negligible. In general, the energy to propagate the crack from a to $a + \mathrm{d}a$ consists of two contributions:

1. the energy to create the new crack surfaces Γ;

2. the energy dissipating in a certain volume around the crack front, U_d.

The energy contribution, U_d, usually highly exceeds the energy necessary for creation of the surfaces, Γ. The crack resistance, R which designates the total energy investment to create a unit area

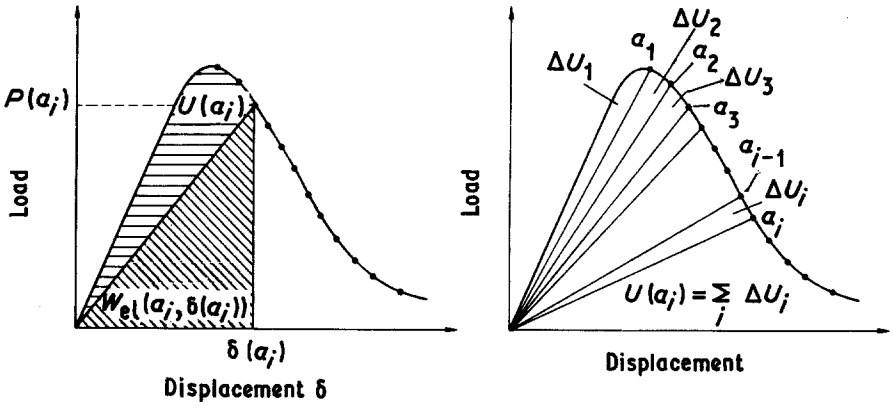

Figure 1 Energy evaluation method (schematic illustration).

of crack surface will be defined as [4]:

$$R = \frac{\partial U_d}{\partial A} + \frac{\partial \Gamma}{\partial A} = \frac{\partial U}{\partial A} \quad (1)$$

For the linear-elastic case as analysed by Griffith [5] that means, when

1. linear and time-independent relations exist between stress and strain at the crack front;

2. the crack surfaces are traction free;

3. using the remote stress, σ_C, and the crack length, a_C, a unique stress intensity value, K_C, can be defined, which represents a material constant in case of critical fracture, the crack resistance R reduces to

$$R_C = \frac{\partial U}{\partial A} = \frac{\partial \Gamma}{\partial A} = G_C,$$

G is the Griffith energy release rate.

In this case the relation holds:

$$R_C = \frac{\partial U}{\partial A} = G_C = \frac{K_C^2}{K'} \quad (2)$$

(E' = Young' modulus, $E' = E$ for plane stress, $E' = E(1-\nu^2)$ for plane strain. According to Equation 2, R, G-curves for the linear elastic case can be calculated

1. by combining corresponding stress values and crack lengths with (K-concept):

$$K_C = \sigma_C a_C^{1/2} Y(a/W) \quad (3)$$

(σ_C = remote stress in case of crack propagation, $Y(a/W)$ = geometrical correction function)

2. from measured or calculated changes in compliance by

$$G_C = \frac{P_C^2}{da} \frac{dC}{da} \quad (4)$$

(P_C = load for stable crack extension, C = compliance).

If the material behaves in a non-linear elastic or elastic plastic manner, that means, if an energy dissipating zone exists at the crack front, e.g. Irwin's plastic zone [6] and with the definition of an effective crack length, a_{eff}, and a non-linear energy release rate G^*, Equation 2 still holds:

$$R_C = \frac{\partial U}{\partial A} = \frac{\partial U_d}{\partial A} + \frac{\partial \Gamma}{\partial A} = G_C^* = \frac{K_{Ceff}^2}{E'} \quad (5)$$

K_{eff} is a K-value calculated from that effective crack length, a_{eff}, thus Equation 3 can still be applied for calculation of R, G^* curves.

The great advantage of an energy consideration is that R-values can be calculated independently of material behaviour by Equation 5, even when the actual crack length and the energy dissipating processes going on at the crack front or in the volume around the crack front are not well known.

2.1. Energy evaluation method

The total energy investment $U(a_i)$ to create crack surfaces for a crack of length a_i in Equation 5 can be evaluated from load–displacement curves, gained in a displacement-controlled experiment (see Fig. 1):

$$U(a_i) = W[\delta(a_i)] - W_{el}[a_i, \delta(a_i)] \quad (6)$$

with

$$W[\delta(a_i)] = \int_0^{\delta'(a_i)} P[\delta(a_i)]\, d\delta$$

(P = load, δ = displacement)

For a crack growth, Δa_i, from a_{i-1} to a_i, the energies ΔU_i are given by the areas included from the extrapolation lines back to the origin (compliance lines). The R-values according to

Equation 5 are then found with the slope of a plot of normalized energies U_i/B over crack lengths, a_i.

Sometimes at high temperatures ceramic materials do not show linear elastic but non-linear elastic or "quasiplastic" behaviour [1, 7, 8]. The question arises, whether the calculation method described above holds for the non-linear elastic (quasiplastic) behaviour of ceramics at high temperatures.

In the special case if creep defomation can be excluded, no zero offset of the compliance lines occurs – the lines always can be extrapolated to the origin. Experimentally this fact cannot be realized, because in real unloading experiments extrusion of second phase [1] or bursting out of grains [9] causes a "crack closure effect" and thus a zero offset of unloading lines.

It should, therefore, be emphasized that the described calculation method can be applied not only to ceramic materials with linear elastic but also to those with non-linear elastic (quasiplastic) behaviour.

3. Experimental details

3.1. Equipment

All experiments were performed in air with a three-point bending device in a closed loop hydraulic testing machine (Fig. 2). The displacement could be directly measured and controlled at the lower surface of the specimen near the notch by a Si_3Ni_4 pushrod (Fig. 3). The various displacement rates ($0.02\,\mu m\,min^{-1} < \delta < 30\,\mu m\,min^{-1}$) could be produced by a function generator.

By some improvements to earlier constructions [1], the compliance of the system could be held very low at $C_M = 0.023 \pm 0.003\,\mu m\,N^{-1}$. In all calculations this system compliance is accounted for. Vibrations of the hydraulic system could be almost completely removed.

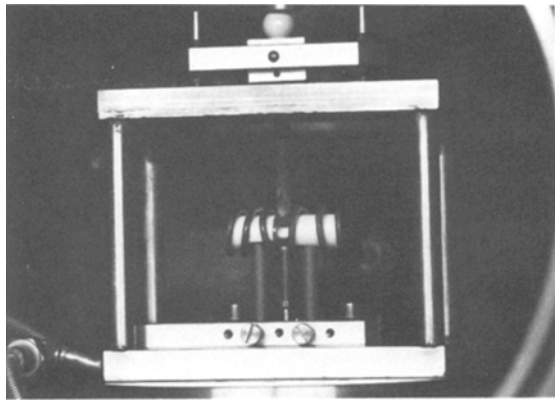

Figure 3 Displacement control unit.

A microscope with photographing, filming or video equipment is attached in such a way that the crack tip could be observed on the specimen surface during the experiments (Fig. 4).

The span of the bending device was 30 mm, the high temperatures were achieved by induction heating of a $MoSi_2$ tube surrounding the specimen. The specimen dimensions were 35 mm × 7 mm × 25 mm.

3.2. Crack length evaluation

3.2.1. Compliance calculation

Crack lengths are calculated from the extrapolated compliance lines by, at least for the linear elastic case, an experimentally well established formula [1, 7, 8, 10]:

$$a_i = a_{i-1} + \frac{W - a_{i-1}}{2} \frac{C_i - C_{i-1}}{C_i} \qquad (7)$$

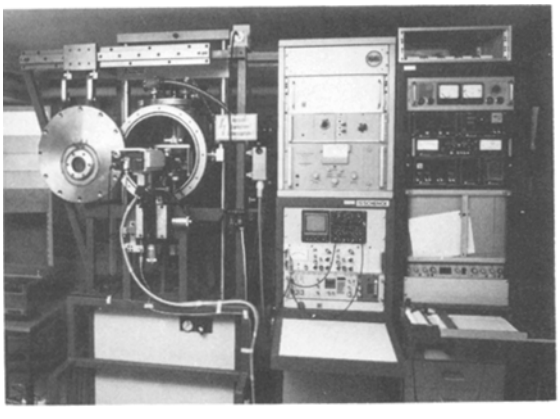

Figure 2 Loading equipment.

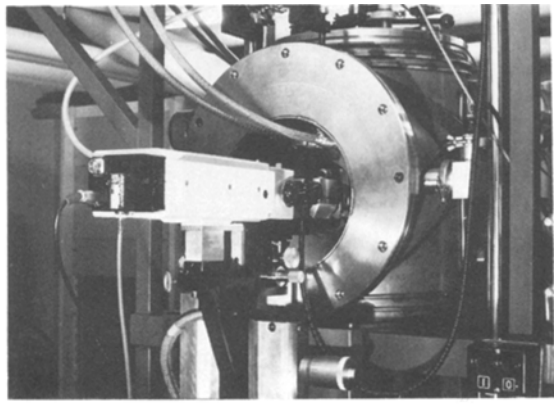

Figure 4 Travelling microscope with video equipment.

TABLE I

	Al_2O_3-r	Al_2O_3-s
Purity (%)	99.7 + 0.3 MgO, SiO_2	97.0 + 3.0 glassy phase
Grain size (μm)	2	11
Density (kg m^{-3})	3.92×10^3	3.68×10^3
Young's modulus (20° C, GPa)	385	342
K_{IC}(20° C) (MPam$^{1/2}$)	3.8 ± 0.4	4.2 ± 0.5

Experimentally the crack lengths are measured directly by watching the crack tip on the specimen surface. At high temperatures this procedure requires rather complicated experimental equipment (see Section 3.1.).

3.2.2. Direct observation

The expanding crack is pursued by a travelling microscope. The crack lengths can be measured directly by a micrometer or on photographs.

Before the maximum load is reached, photographs from the crack tip are taken at a constant time spacing by means of a time switch (in the case of photographing 5 to 50 pictures min^{-1} depending on the loading rate, δ; in the case of filming, a picture is taken every second). This procedure is carried on until the specimen is completely broken. The time spacings are chosen so that a minimum of twenty photographs of the crack tip are available for every experiment. The photographs were put together to obtain an overall view of the complete crack and to fix and measure the actual crack lengths. The observation of the crack tip at the specimen surface involves the problem of crack front curvature over the specimen thickness. This problem was investigated separately [11, 12]. The maximum error in crack length measurement was estimated to be ± 2% from the overall crack length (notch depth plus sharp crack length) and no remarkable crack curvature was found. This backs the opinion that no plastic zone in front of the crack exists as it was found in metallic materials in cases of plain stress and plain strain.

4. Materials

To show the problems arising at high temperatures, two different aluminas were investigated. Their properties are listed in Table I.

A debased alumina containing 3 wt% glassy phase (Al_2O_3-s) was used which served as a model material for non-linear "plastic" reactions at temperatures higher than 800° C. For comparison, measurements were performed with a commercially pure alumina (Al_2O_3-r) which exhibits a linear stress–strain behaviour up to 1000° C.

5. Experiments

5.1. Experiments referring to linear elastic behaviour

The applicability of the energy evaluation method is demonstrated on the fine-grained pure alumina material (Al_2O_3-r in Table I). This material behaves in a completely linear-elastic manner up to high temperatures [1, 7].

Figs. 5a to c give the original load–displacement curves at 20, 900 and 1000° C (unbroken lines). As an example, the broken line in Fig. 5b shows this curve corrected for the system compliance, C_M.

The crack lengths, evaluated by compliance and direct observation (see Section 3.2), coincide for all three temperatures. In the range $10 < \delta < 12\,\mu$m, a small scatter in directly measured crack lengths occurs (Fig. 5b).

For comparison, both crack length evaluation methods where used to caluculate the R-curves from the load-displacement curve of Fig. 5b using Equation 4 (Fig. 6). The scatter in the directly measured crack length effects a scatter in R. Both crack length measurements result in a horizontal R-curve. In addition, if linear elastic behaviour exists, both methods give equal results.

Again for the load–displacement curve of Fig. 5b, the R-curve calculated from the energy concept (Equation 2) is compared in Fig. 7 to the R-curve gained from the stress intensity concept (Equation 3). The K_I-values are calculated from load and corresponding crack lengths, the crack lengths for both curves being the calculated ones. The R-curves for both methods coincide and the values remain constant with increasing crack lengths such as in Fig. 6, as is expected for a linear-elastic material [13].

In conclusion it should be noticed that in the case of linear elastic behaviour

1. the application of the energy and the stress intensity concept results in coinciding R-curves;

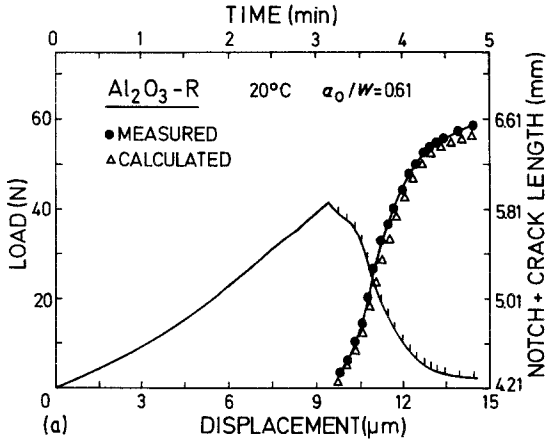

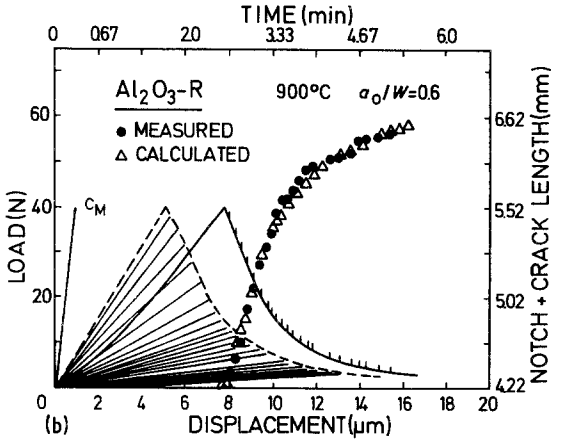

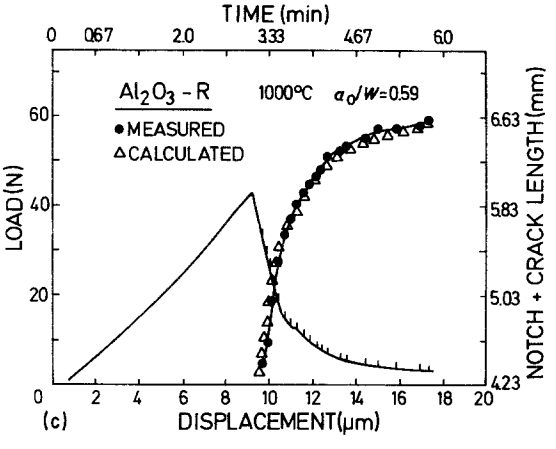

Figure 5 (a) to (c) Load–displacement curves and crack lengths for pure alumina.

2. the R-values are independent of crack length;

3. for experimental reasons the calculated crack lengths may be preferred to the directly measured ones.

5.2. Experiments referring to non-linear elastic (quasiplastic) behaviour

Up to this point in the discussion the behaviour of the materials can be described either by the energy approach in connection with directly measured crack lengths, or with a stress intensity approach if an a_{eff} can be defined (Equation 5).

Linear-elastic behaviour as described above is found for many ceramic materials and glasses at room temperature, for pure alumina materials up to high temperatures of $\simeq 1000°$ C [1, 7, 9]. The reasons for a deviation from linear-elastic behaviour with ceramic materials are different from those found with metals and alloys. Time-dependent creep deformation, which was found, for instance,

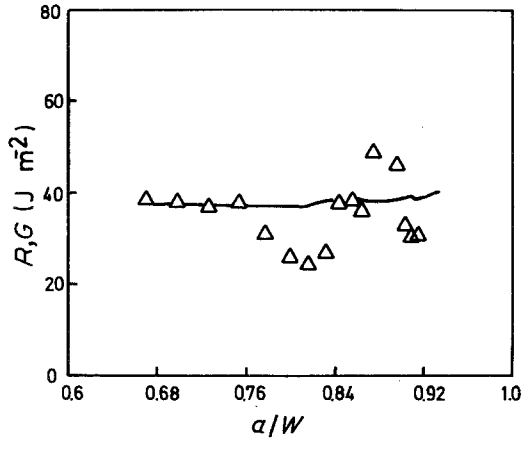

Figure 6 R-curves for the load–displacement curve of Fig. 5b, gained from calculated (unbroken line) and observed crack lengths (triangles).

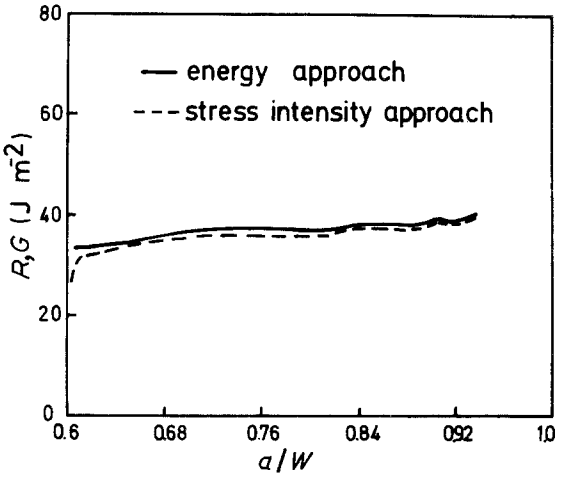

Figure 7 Comparison between the R-curves gained from Fig. 5b, by energy concept (unbroken line) and stress intensity concept (broken line) with calculated crack lengths.

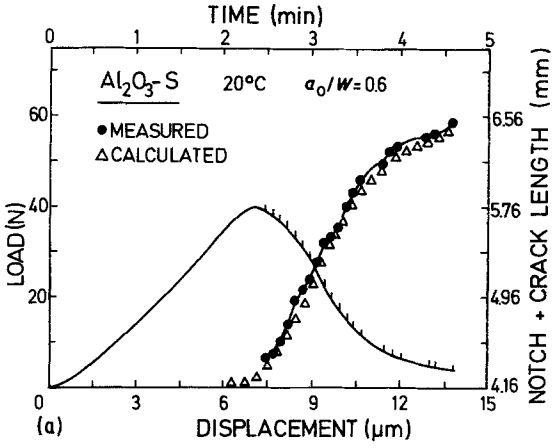

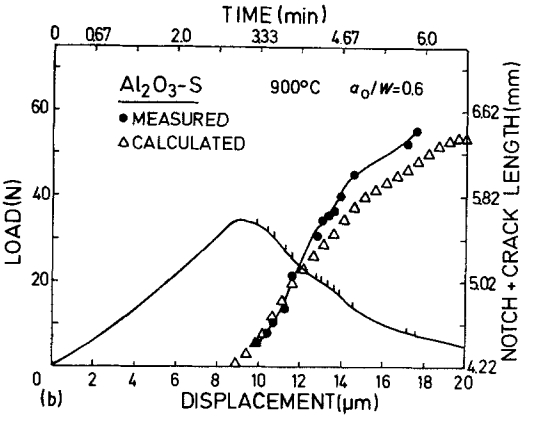

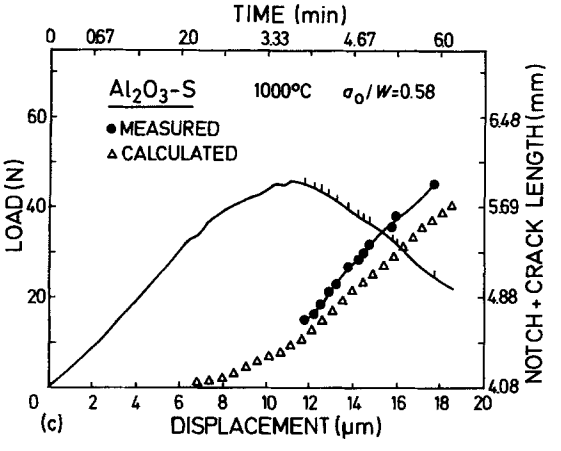

Figure 8 (a) to (c) Load–displacement curves and crack lengths for alumina containing 3% glassy phase.

in special SiSiC materials at high temperatures [14], may be excluded.

According to recent investigations deviations from linear-elastic behaviour in ceramics are caused by the fact that the crack surfaces are found to be not traction free, e.g. for materials containing a second phase, although a linear elastic field in front of the crack still exists [1, 7–9, 15, 16]. If the influence of the tractions can be accounted for – this could be done by a correction of crack length to $a_{\text{eff}} = a_0 + d$ (a_0 = visually measured crack length, d = perturbation zone length) – the stress intensity concept could still be applied.

For the case discussed here, d has to be subtracted and the fictive crack front is to be transferred from the coninuum back behind the visually measured actual crack front.

Two effects may be mainly responsible for forces acting between the crack surfaces behind the crack front:

1. according to direct observations using coarse-grained alumina materials [17], energy dissipative mechanisms caused by friction and microcracking are acting behind the crack front. The R-curves for these materials show a crack length dependence (rising R with crack length) even at room temperature. This behaviour is temperature independent [9, 11, 17];

2. in ceramics containing second phase, for which these phases become viscous at high temperatures, the crack sides adhere together and additional energy investment is to be bought up for crack opening [1, 7].

In both cases, "plastic zones" or "processing zones" in a classical sense cannot be defined, because the energy dissipation processes are treated *behind* the crack front rather than in front of the crack. Nevertheless, although the crack front is in a linear elastic stage, the macroscopic behaviour of these materials seems best described by the energy concept in connection with directly measured crack lengths, as the expression for the stress intensity is actually not known.

Figs. 8a to c show the load–displacement curves at 20, 900 and 1000° C for alumina material containing 3% glassy phase, (Al_2O_3-s in Table I) at a displacement rate of 3 μm min^{-1}. In comparison to Figs. 5a to c (curves for the linear-elastic behaving material), the curves show no sharp load maximum. For the further considerations, Fig. 8a is an exception, because at 20° C the material Al_2O_3-s behaves in a linear-elastic manner like the Al_2O_3-r material in Fig. 5a. The curves in Figs. 8b and c include a larger area than those in Figs. 5b and c. This larger area results from energy dissipating processes during crack extension.

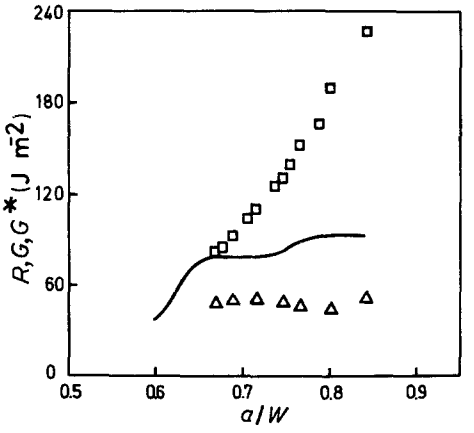

Figure 9 R-curves for the load–displacement curve of Fig. 8c: unbroken line, energy concept; squares, stress intensity concept, linear elastic case; triangles, stress intensity concept, effective crack length, a_{eff}.

The two crack-length evaluation methods result in different crack lengths. For a certain displacement the calculation from compliance "sees" a shorter crack than the direct measurement. This fact indicates that the crack surfaces may not be traction free (see Figs. 8b and c).

As an example, using the load–displacement curve of Fig. 8c, with directly measured crack lengths, the R-curve is calculated from the energy values according to Equations 5 and 6 (Fig. 9). The unbroken line represents the R-curve.

At small crack lengths, a value of $40\,J\,m^{-2}$ is calculated which corresponds to the value for linear elastic behaviour (see Figs. 6 and 7). The crack starts at the first departure from the straight line in the displacement curve (see Fig. 8c). At the maximum load a crack length of $\cong 0.5$ mm has developed.

Correspondingly, the R-data increase from $40\,J\,m^{-2}$ up to $90\,J\,m^{-2}$ (Fig. 9) and then remain constant at that level. When the R-curve reaches its plateau, the adhesive zone behind the crack front has developed its full size and external load and tractions are in a type of dynamic equilibrium. Referring to the example of Fig. 9, the adhesive zone has grown to a length of 0.5 mm. This behaviour is reproducible. For $a/W > 0.8$ disturbances of the ligament by the upper load bearing may occur [7, 18].

If the stress intensity concept for linear-elastic behaviour (Equation 3), again with directly measured crack lengths, is applied, the $R(G)$ values rise to levels that, at least for that special material, cannot be physically justified (square symbols in Fig. 9). If an a_{eff} (measured crack length minus length of adhesive zone) is used, one obtains $R(G^*)$ values on a level of the linear elastic case, independent of crack length (triangular symbols in Fig. 9).

In this special case the crack is transferred back from the continuum to a disturbed zone – the energies necessary for building up the adhesive zone are not accounted for (the triangular symbols in Fig. 9 are on a lower level than the unbroken line). Thus the insert of effective crack lengths and corresponding loads results in K-values for a material without an adhesive zone (Fig. 9). According to this difference in the energy levels evaluated by the energy approach in connection with directly measured crack lengths and alternatively with a stress intensity approach, it can be stated that the special non-linear elastic behaviour cannot be described by a calculated a_{eff}.

6. Comparison of the energy concept to other concepts of non-linear fracture mechanics used for metals

The J-integral concept of elastic–plastic fracture mechanics as was developed for metals in the linear-elastic case leads to a formula corresponding to Equation 2 [19]:

$$|R| = |G_C| = |J| \tag{8}$$

This concept can be extended to the elastic–plastic region up to the full plastic state, if no unloading occurs. A non-linear elastic deformation is assumed to be interchangeable with the elastic–plastic deformation [20].

Earlier investigations concerning the applicability of this concept to ceramic materials at high temperatures were performed for different J-evaluation methods [1–3]. The methods failed for a ceramic material containing a glassy phase, because unloading procedures were necessary for crack length evaluation, which activated the adhesive zones behind the crack front ("crack closure effect") and resulted in rising J_R-curves [1]. In the present case, the theoretical presumptions for J-calculation again do not seem to be fulfilled because:

1. the measurements are performed with a moving crack where relaxation processes at the crack tip may occur;
2. the plastic zone is situated *behind* the crack front;
3. time dependency cannot be excluded.

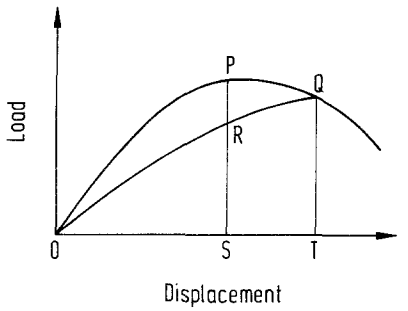

$OPRSO \simeq U_1$ $\quad ORQTSO \simeq U_2$

$OPQRO \simeq U_3$ $\quad PQTSRP \simeq U_4$

$U_1 + U_4 = U_2 + U_3$

Figure 10 J-evaluation method of Garwood (schematic illustration).

Nevertheless the J_R-calculation procedure proposed by Garwood *et al.* [21] for bend specimens was applied to the material Al_2O_3-s:

$$J_i = J_{i-1}\,\frac{BW-A_i}{BW-A_{i-1}} + \frac{2U_4}{BW-A_{i-1}} \qquad (9)$$

The advantage of the calculation of J by this iterative formula is that a determination of the slope $\partial U/\partial A$ in Equation 2 can be avoided. The area U_4 can be seen from Fig. 10.

For the realistic experimental case Equation 2 can be expressed (see Fig. 10) as :

$$R = \frac{\partial U}{\partial A} = \frac{U_3}{A_1 - A_0} \qquad (10)$$

For small crack surface increments, ΔA, there holds [21]:

$$\frac{J_1 + J_0}{2} = \frac{U_3}{A_1 - A_0} \qquad (11)$$

If the simple formula for J, though applicable only for deep cracked bend specimens, is used [22]:

$$J = \frac{2U}{BW-A} \qquad (12)$$

U_1 and U_2 are expressed by this formula:

$$U_1 = \frac{J_0(BW-A_0)}{2};\; U_2 = \frac{J_1(BW-A_1)}{2} \qquad (13)$$

and U_1 and U_2 from Equation 13 and U_3 from Equation 11 are substituted in the sum given in Fig. 10:

$$U_1 + U_4 = U_2 + U_3 \qquad (14)$$

one obtains Equation 9.

For these considerations it is presumed that the value of J is not affected by the way in which Q is reached in Fig. 10. This seems plausible for plastic deformation exceeding the elastic one *in front* of the crack.

For the present ceramic material Al_2O_3-s, referring to the reasons mentioned above, the application of Equation 9 seems dubious. In spite of these doubts, a comparison of the calculation by Garwood's formula with the energy concept used here, in Figs. 11a and b shows convincing agreement. According to further investigations, Garwood's formula presents a useful numerical method for the evaluation of R-curves with ceramic materials [23, 24].

The J_R-calculation procedure given by Garwood is based merely on geometrical considerations. A more general analytical concept for J_R-calculation from a single load-displacement curve with a

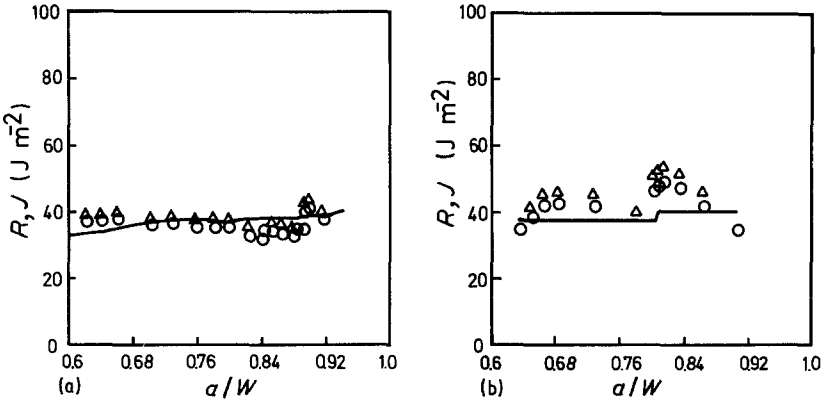

Figure 11 Comparison between the J-evaluation methods of Garwood (triangles), Ernst (circles) and the energy concept (unbroken line), (a) for pure alumina at 900° C, gained from calculated crack lengths of Fig. 5b, (b) for alumina containing 3% glassy phase at 900° C, gained from observed crack lengths of Fig. 8b.

moving crack is given by Ernst *et al.* [25]:

$$J_i = J_{i-1} + \left(\frac{\eta}{b}\right)_{i-1} A_{i-1,i}\left[1 - \left(\frac{\gamma}{b}\right)_{i-1}\right](a_i - a_{i-1}) \tag{15}$$

$A_{i-1,i}$ represents the same area U_4 of Fig. 10 for the ith step, normalized for thickness B.

With $b_{i-1} = W - a_{i-1}$ and the factors $\eta = 2$ and $\gamma = 1$ for three-point bending specimens [25] one obtains the equation:

$$J_i = J_{i-1}\frac{BW - A_i}{BW - A_{i-1}} + \frac{2U_4}{BW - A_{i-1}} \cdot \frac{BW - A_i}{BW - A_{i-1}} \tag{16}$$

Obviously Equation 15 for three-point bending specimens is identical to Garwood's formula, Equation 9, besides a factor $\eta' = BW - A_i/(BW - A_{i-1})$. If the measuring points are chosen close together, this η' differs only slightly from unity ($0.95 < \eta' < 1$) and shows nearly no dependency on normalized crack length a/W.

In Figs. 11a and b this fact is demonstrated, for the values calculated by Ernst's formula are somewhat smaller than those calculated by Garwood's.

In summarizing the results above it should be mentioned that:

1. the energy concept and the J-evaluation methods of Garwood and Ernst give comparable results (see Figs. 11a and b) for ceramic materials containing a second phase at high temperatures in bending experiments;

2. the J-evaluation methods have the advantage of being easily calculable, because they are based on iterative addition of areas, no differentiation is necessary as it is the case with the energy concept;

3. the results by the J-evaluation methods cannot be interpreted according to the definition of the J-integral, because essential presumptions for the J-integral calculation are violated.

7. Conclusions

An apparatus has been developed which allows the direct visual observation of crack extension in ceramic materials at elevated temperatures. The specimens were fractured in a completely displacement-controlled three-point bend test.

The directly measured crack lengths were then compared with those calculated from compliance. From the area under the load-displacement curves and the crack lengths (directly measured and compliance calculated), a crack resistance parameter, R, was evaluated and plotted as a function of normalized crack lengths.

An energy approach R was chosen rather than a stress intensity factor to account for non-linear "plasticity" effects at higher temperatures. The notation J-integral was avoided as the experiments were performed with a moving crack where a stress relaxation process takes place at the crack tip.

In the case of linear elastic behaviour at room temperature and for commercially pure alumina at 900 and 1000° C, flat R-curves were measured. The R-data evaluated from a compliance calculation and the directly measured crack lengths are identical. In these cases the energy approach proves to be equivalent to a stress intensity concept which is based on traction free surfaces.

At elevated temperatures and pronounced plasticity reactions (alumina containing a glassy phase), the two different crack length estimations give values which are no longer identical. The R-data with different evaluation methods are therefore also different.

The R-curve, calculated by the energy approach using directly measured crack lengths, rises to a certain level at small crack lengths, and then remains flat. This initial increase in R is attributed to an adhesive zone of constant size and length developed behind the actual crack tip. A "plastic" zone ahead of the crack tip is excluded and stress and strains in front of the crack prove to be linear elastic.

It is important to note that the crack surfaces are now no longer traction free, as is the case with a Griffith crack with no "plasticity" reactions.

The traction free stress intensity approach in this case is, therefore, no longer valid and gives unrealistic data which increases steeply with increasing crack length (rising crack resistivity curve). Nevertheless, as the field in front of the crack tip may be described by linear elastic equations, an effective stress intensity, K_{eff}, may be formulated whose definition is not yet known. In the simplest case, K_{eff} may be formulated by introducing an effective crack length, a_{eff}.

The comparison of R-data evaluated by the energy approach with J-integral expressions developed for metals gives nearly identical values. These J-integral tests for metals mentioned were also performed using a controlled load–displacement device with a stationary moving crack.

References

1. K. KROMP and R. F. PABST, *J. Amer. Ceram. Soc.* **66** (1983) 107.
2. *Idem, Z. Materialprüf.* **22** (1980) 241.
3. *Idem, Met. Sci.* **3** (1981) 125.
4. J. EFTIS and H. LIEBEWITZ, *Eng. Fract. Mech.* 7 (1975) 101.
5. A. A. GRIFFITH, *Phil. Trans. Roy. Soc., London, Ser. A* **221** (1921) 163.
6. G. R. IRWIN, Proceedings 7th Sagamore Materials Conference, Syracuse University Research Institute (1960) Vol IV, p. 63.
7. A. C. BORNHAUSER, PhD thesis, University of Stuttgart, West Germany (1983).
8. T. HAUG, PhD thesis, University of Stuttgart, West Germany (1984).
9. R. STEINBRECH, R. KNEHANS and W. SCHAARWÄCHTER, *J. Mater. Sci.* **17** (1982).
10. G. A. CLARKE, W. R. ANDREWS, P. C. PARIS and D. W. SHMIDT, *ASTM STP* **590** (1976) 27.
11. H. WIENINGER, PhD thesis, University of Vienna, Austria (1984).
12. H. WIENINGER and R. F. PABST, Proceeding 4th European Conference on Fracture, Leoben, Austria (1982) p. 84.
13. J. M. KRAFT, A. M. SULLIVAN and R. W. BOYLE, Proceedings Crack Propagation Symposium, Cranfield, College of Aeronautics (1961) Vol. 1.
14. K. KROMP, A. C. BORNHAUSER, T. HAUG and R. F. PABST, Fortschritte der Deutschen Keramischen Gesellschaft. 1 (1985), in print.
15. T. HAUG, H. G. SCHMID, A. C. BORNHAUSER and V. GEROLD, 2nd International Conference on Creep and Fracture of Engineering Materials and Structures, Swansea, UK (1984) p. 473.
16. F. W. KLEINLEIN, PhD thesis, University of Erlangen, West Germany (1983).
17. H. WIENINGER, K. KROMP and R. F. PABST, *J. Mater. Sci.* to be published.
18. T. HAUG, personal communication, (1983).
19. J. R. RICE, "Fracture", Vol. 2, edited by H. Liebowitz (Academic Press, New York, 1968) p. 191.
20. D. EFTIS, L. JONES and H. LIEBEWITZ, *Eng. Fract. Mech.* **17** (1975) 491.
21. S. J. GARWOOD, J. N. ROBINSON and C. E. TURNER, *Int. J. Fract.* **11** (1975) 528.
22. J. R. RICE, P. C. PARIS and G. MERKLE, *ASTM, STP* **536** (1973) 241.
23. T. HAUG and A. C. BORNHAUSER, *J. Mater. Sci.* to be published.
24. W. VOGEL, personal communication, (1984).
25. H. A. ERNST, P. C. PARIS and J. D. LANDES, *ASTM STP* **743** (1981) 476.

Received 31 July
and accepted 8 October 1984